Research Article

Production and characterization of brake pad developed from coconut shell reinforcement material using central composite design

J. Abutu[1] · S. A. Lawal[1] · M. B. Ndaliman[1] · R. A. Lafia-Araga[2] · O. Adedipe[1] · I. A. Choudhury[3]

Abstract

In this work, locally sourced non-hazardous materials were used to produce brake pad using grey relational analysis (GRA) and experimental design via central composite design. Raw materials selected for production include coconut shell, epoxy resin (binder), graphite (friction modifier) and aluminum oxide (abrasive). Twenty-seven samples were produced separately using coconut shell as reinforcement material by varying process parameters. Formulation of the brake pads samples was done using rule of mixture and a weight percent of 52% reinforcement material, 35% binder, 8% abrasive and 5% friction modifier were used for the production. Grey relational analysis (GRA) shows that optimal process performance can be obtained using molding pressure, molding temperature, curing time and heat treatment time of 14 MPa, 140 °C, 8 min and 5 h, respectively. Optimized sample was produced using the optimal set of process parameters obtained from GRA and compared with commercially available sample produced by Ibeto Group. The experimental results showed that the performance of the optimized coconut shell-reinforced brake pad compared satisfactorily with commercially available samples and capable of producing less brake noise and vibration during application. Analysis of variance shows that curing time with a contribution of 30.38% and 31.40% have the most significant effect on the hardness and ultimate tensile strength of the coconut shell-reinforced friction material, respectively, while heat treatment time with a contribution of 46.3% and 24.23% have the most significant effect on the wear rate and friction coefficient of coconut shell-reinforced brake pad, respectively. The effects of all the factors on the properties of the friction materials are significant since their *p* values are greater than 0.010 (1%).

Keywords Brake pads · Central composite design · Grey relational analysis · Coconut shell and characterization

List of symbols

α	Axial value
μ	Coefficient of friction
β	Distinguishing coefficient
u	Percentage weight
δ	Densities
f	Volume fraction
X	Weight
F	Applied load
d	Disk diameter
t	Time of exposure of specimen to abrasion
N	Radial speed
b	Support span (mm)
t	Specimen thickness (mm)
∂	Deflection (mm)
w	Specimen width (mm)
χ	Distinguishing coefficient
n	Number of factor level combination
k	Performance value
MT	Molding temperature
MP	Molding pressure
CT	Curing time
HTT	Heat treatment time

✉ J. Abutu, joe4abutu@gmail.com | [1]Department of Mechanical Engineering, School of Engineering and Engineering Technology, Federal University of Technology, Minna, Nigeria. [2]Department of Chemistry, School of Physical Sciences, Federal University of Technology, Minna, Nigeria. [3]Department of Mechanical Engineering, Faculty of Engineering, University of Malaya, 50603 Kuala Lumpur, Malaysia.

SN Applied Sciences (2019) 1:82 | https://doi.org/10.1007/s42452-018-0084-x

Received: 17 August 2018 / Accepted: 26 November 2018

Published online: 05 December 2018

1 Introduction

Over the years, disk brake system has been used for safe retardation or deceleration of automobiles. This system consists of three major parts which include the brake pad, rotor and caliper [1, 2]. Belhocine and Nouby [3] revealed that braking system is one of the most fundamental safety components in modern passenger cars as it is significant in stopping or slowing down of vehicles. Brake pads are used in the braking and transmission of various machinery as well as equipment such as aircraft, cars, motorcycles and other automobile vehicles. Their compositions keep on changing in order to meet up with the growing technology and requirements of the environment. Brake pads can be categorized as metallic, semi-metallic, organic and carbon-based, depending on the composition of the constituent elements. Similarly, automobile mechanics are most times exposed to asbestos dust in several ways especially during repair of friction materials, where accumulated dusts are being wiped off before the old pads or shoes are replaced using a brush. This processes put the mechanics at the risk of contracting diseases such as pleural, peritoneal or pericardial mesothelioma, asbestos-related cancer and asbestosis. Rabia et al. [4], also reported that during disk brake engagement, brake pads rub against the brake disk, thereby dissipating kinetic energy in the friction process as a heat. This kinetic energy is transferred into the energy of the contact particles, asperities and atoms which further translates into vibration, thereby generating sound wave [5]. Therefore, to reduce brake noise and vibration during braking, brake pad materials are required to provide low wear rate and stable coefficient of friction at various operating temperatures, pressures, speeds, and environmental conditions [4].

Belhocine [6], used finite element approach to investigate the thermal effects of a disk–pad assembly in the contact behavior and structural performance of the disk–pad model. Three pad designs were simulated in order to identify its influence on the distribution of stresses. The results showed a larger deformation at the outer radius of the disk and unfavorably mechanical behavior of a brake due to the presence of grooves in the samples. In a related research, Belhocine and Wan [7], used CFD (Computational Fluid Dynamics) analysis to generate an approximate description of the behavior of a physical model and to calculate the heat transfer coefficient (*h*) of the full and ventilated brake disks as a function of time. The results indicated that all the values obtained from the analysis were lower than the allowable values. As a result, the authors concluded that the design of disk brake plays a major role in heat transfer and also that gray cast iron is the most suitable material to be in the design of brake disk. In addition, Blau [31] reported that brake pads are composed of four components, which include reinforcements, binders, friction modifiers and abrasives. Several studies have also been carried out with the aim of replacing asbestos and other carcinogenic materials in automobile brake pads using different constituent materials and experimental design techniques. In the work of Anon [8], Norton [9] and Ole-Von et al. [10], the use of antimony in friction materials was investigated and the results showed that the use of antimony (Sb) in friction materials should be suspended as it posed a human cancer risk due to considerable concentrations of Sb in the material. Also, Lawal et al. [11] as well as Ibhadode and Dagwa [12], have used Taguchi experimental design methods to investigate the use of rubber scraps and palm kernel shells, respectively, as reinforcement materials in brake pads production. Also, Ikpambese et al. [13], Aigbodion et al. [14], Idris et al. [15], Ademoh and Adeyemi [16] and Bala et al. [17] utilized trial and error design technique to study the use of palm kernel fibers, bagasse, banana peels, maize husk and cow hooves, respectively, as reinforcement in brake pads production. The results presented by the authors indicated that the performance of the selected non-hazardous reinforcement materials were closely comparable with other commercially available pads and, as a result, may serve as a substitute for asbestos.

Abutu et al. [18], also investigated the use of seashell (reinforcement material) as possible alternative for asbestos in brake pad production by utilizing experimental design technique (Central Composite-RSM design) and multi-response optimization technique (Grey Relational Analysis). The authors reported that optimal performance of the developed brake pad can be achieved using molding pressure (MP), molding temperature (MT), curing time (CT) and heat treatment time (HTT) of 14 MPa, 160 °C, 12 min and 1 h, respectively. However, in this study, the effect of coconut shell inclusion in brake pad production using similar experimental conditions and technique adopted in the work of Abutu et al. [18] was investigated. The seashell utilized as reinforcement material by the authors was substituted with coconut shell in order to examine the effects of the material (coconut shell) on the performance of the brake pad. In addition, fewer materials (coconut shells, graphite, epoxy resin and aluminum oxide) were used in this study as against 10–25 ingredients used by other researchers to develop brake pads [14, 16, 19]. Presently, environmental concerns have motivated the demand for biodegradable materials such as plant-based natural fiber reinforcement materials in composites manufacturing. These composites are fast replacing conventional materials in many applications, especially

in automobiles, where tribology (friction, lubrication and wear) is important. Also, plant fiber resources are renewable, widely distributed, locally available, moldable, anisotropic, versatile, non-abrasive, porous, easily available in many forms, biodegradable, combustible, compostable and reactive. It has a high aspect ratio, high strength-to-weight ratio and has good insulation properties (sound, electrical and thermal). Some of these properties such as biodegradability and combustibility which might be considered as shortcomings are actually features providing a means of predictable and programmable disposal that is not easily achieved with other resources [20]. As a result, coconut shell reinforcement in brake pad production provides a better alternative to asbestos in terms of better environmental blueprint.

Statistical method such as central composite experimental design (CCD) and grey relational analysis (GRA) were also utilized for experimental design and multi-response optimization, respectively. These techniques are against the usual Taguchi design as well trial and error method used in previous reports. The tribological and mechanical properties of the developed and commercial(control) brake pad samples were investigated using the testing conditions adopted by Abutu et al. [18] and the results (responses) obtained were discussed. The application of coconut shell as reinforcement material will serve as a means of utilizing agricultural wastes and also contribute to the actualization of the local content initiative for the use of locally made products in indigenous automobile industries in Nigeria.

2 Materials and methods

2.1 Materials

Coconut shell (Fig. 1), obtained from a coconut trader in Sabon Tasha market in Kaduna—Nigeria was used as material for reinforcement while graphite powder sourced from used 1.5 V TIGER head dry cell batteries was utilized as a friction modifier and alumina (Cat. No. 34143; Lot. No. 44100), purchased from a commercial chemical store in Onitsha-Nigeria was used as abrasive material. Also, Epoxy resin (Epoblock, FIP Chemicals), obtained from a chemical store in Onitsha-Nigeria was used jointly with a hardener (Sikadur 42T, Sika Corporation U.S.) to serve as binder.

Fig. 1 Crushed coconut shells

2.2 Method

Several processes were involved in the development of coconut shell-reinforced brake pads composite. This includes the formulation of composite using rule of mixture principle, preparation of fillers (graphite and coconut shell powder), design of experiment using central composite design (CCD), compression molding process, post-curing, tribological and mechanical examination as well as optimization using grey relational analysis (GRA). The coconut shell and graphite powder were prepared using the preparation method adopted by Norazlina et al. [21].

2.2.1 Preparation of materials and formulation of samples

The preparation of the coconut shell and graphite powder involved removing of the shell fibers, washing with soap and detergent, cleaning using dried cloth, drying in a hot air oven operating at a temperature of 150 °C for 2 h, followed by crushing with mortar and pestle. Other preparation process includes grinding of the crushed shells with grinder and finally sieving using a sieve size of 125 µm. Rule of mixture was used to formulate the brake pad samples. To use this theorem efficiently, the density (δ) and volume fraction (f) of the individual constituents were calculated using a specified weight percent. The volume fraction (f) of individual constituent for the coconut shell-reinforced composite was calculated using Eq. 1, whereas Archimede's principle was used to determine the densities of coconut shell and graphite while the densities of reagent grade aluminum oxide and epoxy resin were provided by the producers [18, 22].

$$\text{Volume Fraction}\left(f_i\right) = \frac{u_i}{\delta_i} \div \sum \frac{u_j}{\delta_j} \tag{1}$$

u_j and u_i are the percentage weight of the total and individual constituent, respectively, while δ_j and δ_i are the densities of the total and individual constituents, respectively. f_i is the volume fraction of the individual constituent. Therefore, the theoretical density of the coconut shell-reinforced brake pads is shown in Eq. 2 [18, 22].

$$\delta_{\text{(Coconut Shell - based)}} = \delta_g f_g + \delta_b f_b + \delta_c f_c + \delta_a f_a \tag{2}$$

f_g, f_c, f_b and f_a, are the volume fraction of the graphite, coconut shell, epoxy resin and aluminum oxide, respectively.

δ_c, δ_a, δ_g and δ_b are the densities of the coconut shell, aluminum oxide, graphite and epoxy resin, respectively.

2.2.2 Design of experiment

Experimental design was done using response surface methodology (RSM) via central composite design (CCD). This design technique consists of two-level full factorial design; axial and center points. This design matrix was built using Minitab 17 software in accordance with standard RSM's $L_{27}(2)^4$ as shown in Table 1. MT (molding temperature), MP (molding pressure), CT (curing time) and HTT (heat treatment time) were chosen as the process factors used in analyzing its effects on the performance of the brake pads. Table 2 shows the experimental Matrix for the Design Layout.

2.2.3 Production of brake pad samples

Samples production was carried out on a compression molding machine (Model; 0577-86365889, Wenzhou Zhiguang Shoe-Making Machine Co. Ltd), using standard procedure specified and adopted by Abutu et al. [18] and Chemiplastica

Table 1 Factor levels for process factors

Factors	Unit	Center point	Axial points		Cubic points	
		0	Upper level (+ 2)	Lower level (− 2)	Upper level (+ 1)	Lower level (− 1)
Molding pressure (MP)	MPa	14	18	10	16	12
Molding temperature (MT)	°C	140	180	100	160	120
Curing time (CT)	min	8	12	4	10.0	6.0
Heat treatment time (HTT)	h	3	5	1	4.0	2.0

Table 2 Experimental matrix for RSM—central composite design layout

Run	Design layout				Experimental design matrix			
	MP (MPa)	MT (°C)	CT (min)	HTT (h)	MP (MPa)	MT (°C)	CT (min)	HTT (h)
1	−1	−1	−1	−1	12	120	6	2
2	1	−1	−1	−1	16	120	6	2
3	−1	1	−1	−1	12	160	6	2
4	1	1	−1	−1	16	160	6	2
5	−1	−1	1	−1	12	120	10	2
6	1	−1	1	−1	16	120	10	2
7	−1	1	1	−1	12	160	10	2
8	1	1	1	−1	16	160	10	2
9	−1	−1	−1	1	12	120	6	4
10	1	−1	−1	1	16	120	6	4
11	−1	1	−1	1	12	160	6	4
12	1	1	−1	1	16	160	6	4
13	−1	−1	1	1	12	120	10	4
14	1	−1	1	1	16	120	10	4
15	−1	1	1	1	12	160	10	4
16	1	1	1	1	16	160	10	4
17	−2	0	0	0	10	140	8	3
18	2	0	0	0	18	140	8	3
19	0	−2	0	0	14	100	8	3
20	0	2	0	0	14	180	8	3
21	0	0	−2	0	14	140	4	3
22	0	0	2	0	14	140	12	3
23	0	0	0	−2	14	140	8	1
24	0	0	0	2	14	140	8	5
25	0	0	0	0	14	140	8	3
26	0	0	0	0	14	140	8	3
27	0	0	0	0	14	140	8	3

[23]. During the process, samples composition formulated using rule of mixture remained constant throughout the production, while the process factors (MP, MT, CT and HTT) were varied as shown in Table 2. As specified by Chemiplastica [23], initial preparation involved pouring 23.33% (41.06 g) of the epoxy resin into a container followed by the addition of 11.67% (20.54 g) of hardener in the proportion of 2:1. The mixture of the hardener and epoxy resin were manually stirred in a separate container until a homogenous mixture was obtained. The weighed portion of the fillers (coconut shell, alumina and graphite) was also mixed manually in another separate container. The overall mixture was stirred thoroughly in order to attain a consistent blend and was transferred into the mold for compression molding. The final stage of production involved subjecting the molded products to a temperature of 150 °C in a hot air oven (Fig. 2) for further heat treatment at varying times as presented in Table 2.

2.2.4 Characterization of samples

Sample characterization was carried out in accordance with the testing method adopted by Abutu et al. [18]. The properties investigated during this study as well as the testing procedures are discussed as follows;

(1) Coefficient of friction

This test procedure was carried out in accordance with Standard Organization of Nigeria (S.O.N) [16] recommended test practice using an inclined angle (α) tilted and fixed at 15° as shown in Fig. 3. The weight, (F), of the specimen attached to the steel plate and their respective coefficient of friction were calculated using Eqs. 3 and 4.

$$F = m\,(\text{mass}) \times a\,(\text{acceleration due to gravity}) = m \times g \tag{3}$$

$$\text{Coefficient of friction}\,(\mu) = \frac{F - X\text{Sin}\alpha}{X\text{Cos}\alpha} \tag{4}$$

Fig. 2 Heat-treated coconut shell-reinforced brake pad samples

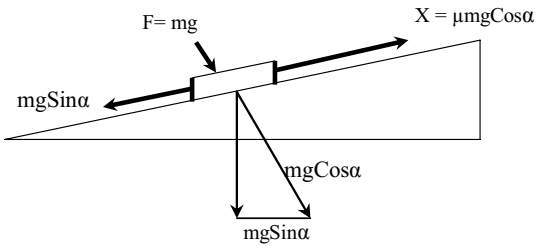

Fig. 3 Analysis of friction coefficient

where α angle of inclination in degree; X weight of mild steel plate and test specimen and F applied load (frictional force).

(2) Wear rate

Wear rate of samples produced using RSM-CCD experimental design was conducted using a Martindale abrasion testing machine (SATRA TECHNOLOGY, S/N: 11884, Supply-230-1-50, STM: 105) with operating speed of 50 rev/min, pre-set cycle of 1000 in 1200 s and pressure of 1.2603 MPa applied at constant speed (50 rev/min). The sliding distance (D) and wear rate (W_r) were calculated using Eqs. 5 and 6 [18]. Also, the wear rate of commercial (control) and optimized samples produced using multi-response technique (GRA) was studied using a Tribometer (ANTON PAAR GmbH, CSM Instrument, Strasse 20, 8054 Graz—Austria) operating at a speed of 10 cm/s and applied load of 7 N.

$$\text{Sliding distance}\,(D) = 2\pi Ndt \tag{5}$$

$$W_r = \frac{\text{Loss in weight}\,(w_l)}{\text{Sliding distance}\,(D)} \tag{6}$$

where d, t and N, disk diameter, time of exposure of specimen to abrasion and radial speed, respectively.

(3) Ultimate tensile strength (UTS)

A Tensometer (MONSANTO; Serial No-05232) with loading beam of 600 N was used to determine the UTS of the friction materials. This test was carried out in accordance with ASTM D638 type IV standard with specimen prepared as shown in Fig. 4. The experimental results obtained were used in calculating the UTS, percentage elongation, and young modulus using the Eqs. 7, 8 and 9, respectively [18].

$$\text{Percentage elongation} = \frac{\text{change in length}\,(e)}{\text{Initial guage length}\,(i_o)} \times 100 \tag{7}$$

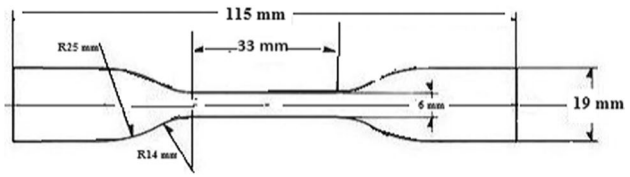

Fig. 4 ASTM D638 dumbbell shape and dimension

$$\text{UTS (MPa)} = \frac{\text{Maximum load}}{\text{Cross Sectional Area}} \quad (8)$$

$$\text{Young Modulus } (\gamma) = \frac{\text{UTS}}{\text{Elongation}} \quad (9)$$

(4) Compressive strength

Compressive strength of the friction materials was determined using universal testing machine (ENERPAC P391: Cat. Nr. 261, Norwood Instruments Ltd., Great Britain) with a 100 kN Capacity. Three specimens from each sample were tested in accordance with ASTM D695 testing standard. The deflection as well as the load at which specimen failure occurred was recorded and the average value calculated for each test sample. The compressive strength and total surface area of the specimen were calculated using Eqs. 10 and 11, respectively, [18].

$$\text{Compressive Strength (CS)} = \frac{\text{Maximum breaking load } (L)}{\text{Total surface area } (S_a)} \quad (10)$$

$$\text{Total surface area } (S_a) = 2(wh + bt + ht) \quad (11)$$

where t, w and h are the thickness, width and height of specimen, respectively.

(5) Hardness

Hardness test was carried out in accordance with ASTM D2240 type D scale standard using a loading force of 44.73 N and specimen thickness of 6 mm. This experiment was conducted using a Durometer hardness tester (FRANCISCO, Model: 5019, Shore D Scale, Munoz Irles C. B; S/N: 01554). The hardness values at three test points from different test samples were recorded and the average results calculated.

(6) Flexural strength

The flexural test was conducted using a universal testing machine (ENERPAC P391: Cat. Nr. 261, Norwood Instruments Ltd., Great Britain, 100 kN Capacity) and specimens were prepared to a size of 80 × 15 × 10 mm and tested in accordance with ISO 178:2003 standard which also specified a test span of 60 mm. The breaking load as well as deflection readings was recorded, while the flexural strain, stress and modulus were calculated using Eqs. 12–14 [18].

$$\text{Flexural stress, } (\sigma_f) = \frac{3Fb}{2wt^2} \quad (12)$$

$$\text{Flexural strain, } (\lambda_f) = \frac{6\partial t}{b^2} \quad (13)$$

$$\text{Flexural Modulus, } (\gamma_f) = \frac{Fb^3}{4w\delta t^3} = \frac{\text{Flexural Stress } (\sigma)}{\text{Flexural Strain } (\lambda)} \quad (14)$$

where w width of test specimen, b support span (mm), t specimen thickness (mm), ∂ deflection (mm), F applied load to fracture the specimen (kN) and w specimen width (mm)

(7) Impact strength test

Impact test was conducted in accordance with ASTM E23 testing procedure using an impact testing machine (Norwood instrument, model No: 412-07-0715269C) in Charpy mode. Test specimens were prepared in accordance with ASTM E23 test standard which specified a specimen size of 55 × 10 × 10 mm with notch angle 45°, 0.25 mm notch radius and 2 mm notch depth along the base. The impact strength of each brake pad sample was calculated using Eq. 15 [18, 24].

$$\text{Impact Strength } (I_s) = \frac{\text{Energy absorbed}}{\text{Specimen thickness } (t)} \text{ (J/mm)} \quad (15)$$

3 Results and discussion

3.1 Formulation of samples using rule of mixture

The results of rule of mixture formulation indicate that the coconut shell-reinforced composite has a theoretical density of 1.073 g/cm^3. This predicted value of the brake pad composite is in good agreement with recommended values of commercial brake pad whose densities fall between 1.010 and 2.060 g/cm^3 as reported by Abutu et al. [18] and Efendy et al. [25].

3.2 Experimental results

The results of the tribological and mechanical properties of the developed brake pad samples as well as the signal to noise (S/N) ratio values of individual responses are shown in Table 3. Larger-the-better and smaller-the-better quality characteristics shown in Eqs. 16 and 17,

Table 3 Experimental results and *S/N* ratio values

Run	Coefficient of friction (μ)		Wear rate (W_r)		Ultimate tensile strength (UTS)		Compressive strength (C_S)		Hardness (H)		Flexural strength (F_S)		Impact strength (I_S)	
	Coefficient of friction (μ)	*S/N* (η) ratio (dB)	Wear rate (mg/m)	*S/N* (η) ratio (dB)	UTS (MPa)	*S/N* (η) ratio (dB)	Compressive strength (MPa)	*S/N* (η) ratio (dB)	Hardness (shore D)	*S/N* (η) ratio (dB)	Flexural strength (MPa)	*S/N* (η) ratio (dB)	Impact strength (J/mm)	*S/N* (η) ratio (dB)
1	0.788	−2.07	0.2620	11.64	4.0327	12.11	2.695	8.61	64.67	36.21	13.040	22.31	0.0283	−30.96
2	0.652	−3.72	1.0936	−0.78	3.1059	9.840	3.099	9.82	64.33	36.17	12.700	22.07	0.0238	−32.47
3	0.686	−3.27	0.1310	17.66	5.7021	15.12	3.457	10.77	64.00	36.12	21.929	26.82	0.0305	−30.31
4	0.688	−3.25	0.1703	15.38	2.8468	9.090	3.068	9.74	59.67	35.52	11.902	21.51	0.0233	−32.65
5	0.685	−3.29	0.2030	13.85	7.7895	17.83	5.309	14.50	74.67	37.46	20.174	26.10	0.0294	−30.63
6	0.601	−4.42	0.1244	18.10	2.7575	8.810	2.838	9.06	60.33	35.61	13.690	22.73	0.0276	−31.18
7	0.601	−4.42	0.3995	7.970	4.5601	13.18	3.160	9.99	64.67	36.21	9.538	19.59	0.0248	−32.11
8	0.651	−3.73	0.0393	28.11	3.6547	11.26	3.659	11.27	68.33	36.69	12.990	22.27	0.0280	−31.06
9	0.566	−4.94	0.6614	3.590	0.8747	−1.16	1.802	5.12	53.33	34.54	6.813	16.67	0.0207	−33.68
10	0.533	−5.47	0.2161	13.31	5.2258	14.36	4.698	13.44	56.67	35.07	19.647	25.87	0.0320	−29.90
11	0.688	−3.25	0.0720	22.85	5.8161	15.29	3.284	10.33	61.33	35.75	7.036	16.95	0.0284	−30.93
12	0.496	−6.09	0.0655	23.68	1.8773	5.470	2.864	9.14	60.00	35.56	4.946	13.88	0.0211	−33.51
13	0.558	−5.07	0.6549	3.677	5.6496	15.04	4.279	12.63	67.33	36.56	16.721	24.46	0.0370	−28.64
14	0.649	−3.76	0.7138	2.928	4.9981	13.98	4.580	13.22	58.33	35.32	7.084	17.01	0.0272	−31.31
15	0.568	−4.91	0.6680	3.505	1.3199	2.410	4.834	13.69	60.67	35.66	14.129	23.00	0.0301	−30.43
16	0.477	−6.43	0.7204	2.849	1.6159	4.170	1.098	0.81	74.33	37.42	18.323	25.26	0.0384	−28.31
17	0.668	−3.50	0.1441	16.83	5.7807	15.24	3.323	10.43	59.33	35.47	6.863	16.73	0.0258	−31.77
18	0.571	−4.87	0.0720	22.85	5.7723	15.23	4.44	12.95	58.33	35.32	10.919	20.76	0.0293	−30.66
19	0.617	−4.19	0.6483	3.764	4.2347	12.54	4.391	12.85	60.33	35.61	13.181	22.40	0.0289	−30.78
20	0.648	−3.77	0.0589	24.59	6.7184	16.55	2.791	8.92	62.33	35.89	8.312	18.39	0.0300	−30.46
21	0.650	−3.74	0.0197	34.13	1.9326	5.720	3.209	10.13	60.67	35.66	5.551	14.89	0.0197	−34.11
22	0.550	−5.19	0.0786	22.09	5.8028	15.27	3.189	10.07	63.67	36.08	12.818	22.16	0.0283	−30.96
23	0.720	−2.85	0.0066	43.68	6.861	16.73	4.458	12.98	64.67	36.21	13.262	22.45	0.0291	−30.72
24	0.614	−4.24	0.0720	22.85	7.3792	17.36	4.137	12.33	74.33	37.42	18.344	25.27	0.0341	−29.35
25	0.503	−5.97	0.7138	2.928	6.2296	15.89	4.915	13.83	71.33	37.07	15.352	23.72	0.0318	−29.95
26	0.528	−5.55	0.8382	1.533	7.0795	17.00	5.297	14.48	70.33	36.94	14.188	23.04	0.0309	−30.20
27	0.521	−5.66	0.7924	2.021	6.6499	16.46	4.952	13.90	70.67	36.98	14.692	23.34	0.0337	−29.45

respectively, were used to calculate the *S/N* ratios of the responses. Wear rate was calculated using smaller-the-better quality characteristics (Eq. 17), while friction coefficient and mechanical properties (hardness, UTS, flexural, impact and compressive strength) were calculated using larger-the better quality characteristics (Eq. 16).

$$\text{Larger - the better}: S/N = -10\log\frac{1}{n}\left(\sum_{i=1}^{n}\frac{1}{k^2}\right) \tag{16}$$

$$\text{Smaller - the better}: S/N = -10\log\frac{1}{n}\left(\sum_{i=1}^{n}k_i^2\right) \tag{17}$$

k given factor level combination responses and *n* number of factor level combination.

From the experimental results presented in Table 3, it can be observed that the properties of the friction materials vary as process factors (MP, MT, CT and HTT) changes. The values of friction coefficient and wear rate varies from 0.477–0.788 to 0.0066–1.0936 mg/m, respectively, while UTS, compressive strength, hardness, flexural and impact strength of the brake pads varies from 0.8747–7.7895 MPa, 1.098–5.309 MPa, 53.33–74.67 shore D scale, 4.946–21.93 MPa and 0.01984 to 0.0384 J/mm, respectively. This implies that the developed brake pads possess good mechanical and tribological properties as the results are in close agreement with the earlier work of Bala et al. [17], Ademoh and Adeyemi [16] and Dagwa and Ibhadode [26] who reported hardness and ultimate tensile strength of 72.67 (shore D scale) and 7 MPa, respectively, for commercial-based brake pads. Belhocine and Wan [27], reported that the presence of grooves in brake pads pose negative effects on its mechanical properties, as a result, the absence of groove in developed brake pad samples may be responsible for the good mechanical properties exhibited by the samples. Also, compared to the earlier work of Abutu et al. [18], whose optimal friction coefficient falls within the class G (0.45–0.55), the coefficient of friction of the developed brake pad falls within the class G (0.45–0.55) and H (> 0.55) type of brake pads recommended for use in automobile by the Society of Automobile Engineers (SAE), while the results of wear rate are comparable with the earlier work of Idris et al. [15], who reported a wear rate 3.8 mg/m for commercial-based pads. Similarly, the result of friction coefficient agrees with the findings of Mohd et al. [2] who with the aim of avoiding vehicle from rolling away during operation, established a validated parking brake model and found out those vehicles whose brake pad possesses a friction coefficient (μ) greater than 0.2 will not roll away during application. In another report, Belhocine et al. [28] stated that brake pads with higher coefficient of friction tend to generate more brake power, therefore, pads with higher friction coefficient, possess better ability to slow down the brake disk by the friction forces which opposes its movement during application.

3.3 Grey relational analysis (GRA)

GRA was conducted using procedure outlined in the work of Abutu et al. [18] and Yiyo et al. [29]. This procedure includes calculating the grey relational generation (GRG) with smaller- and larger-the better attributes given in Eqs. 18 and 19, respectively, using the values of *S/N* ratios for individual responses shown in Table 3. This procedure is followed by scaling all performance values to 0, 1 (reference sequence definition) after which the grey relational coefficient (GRC) and grades were calculated using Eqs. 20 and 21, respectively. The final process of GRA is the determination of optimal process factors for the single response.

$$\text{Smaller} - \text{the better attribute}\,(y_{ij}) = \frac{\overline{k}_{ij} - k_{ij}}{\overline{k}_j - \underline{k}_j} \tag{18}$$

$$\text{Larger} - \text{the better attributes}\,(y_{ij}) = \frac{k_{ij} - \underline{k}_i}{\overline{k}_i - k_j} \tag{19}$$

$$(i = 1, 2, 3, 4 \ldots m \text{ and } j = 1, 2, 3, 4 \ldots n)$$

where $k_i = (k_{i1}, k_{i2}, \ldots, k_{ij}, \ldots, k_{in})$, k_{ij} = the performance value of attribute j of alternative i and $\overline{k}_j = \max\{k_{ij}, i = 1, 2, \ldots, m\}$ and $\underline{k}_j = \min\{k_{ij}, i = 1, 2, \ldots, m\}$.

$$\gamma\,(y_{oj}, y_{ij}) = \frac{\Delta_{\min} + \chi\Delta_{\max}}{\Delta_{ij} + \chi\Delta_{\max}} \quad (i = 1, 2, \ldots, m \text{ and } j = 1, 2, \ldots, n) \tag{20}$$

where χ is the distinguishing coefficient and 0.5 is the widely accepted value [18, 30].

$\Delta_{ij} = y_{0j} - y_{ij}$, $\Delta_{\min} = \min(\Delta_{ij}, i = 1, 2, \ldots, m; j = 1, 2, \ldots, n)$ and $\Delta_{\max} = \max(\Delta_{ij}, i = 1, 2, \ldots, m; j = 1, 2, \ldots, n)$, $\gamma\,(y_{0j}, y_{ij})$ is the GRC between y_{ij} and y_{0j}, $X \in [0, 1]$ and $\Delta_{\max} = \max(\Delta_{ij}, i = 1, 2, \ldots, m; j = 1, 2, \ldots, n)$. Abutu et al. [18] reported that after GRG, $\Delta_{\max}$ will be equal to 1 and $\Delta_{\min}$ will be equal to 0.

$$\phi(y_0, y_i) = \sum_{j=1}^{n} w_j \beta\left(y_{oj}, y_{ij}\right); \quad (i = 1, 2, 3 \ldots m) \tag{21}$$

w_j represent the weight of attribute j which is usually dependent on the judgments of the decision maker or the

structure of the proposed problem. Abutu et al. [18] and Yiyo et al. [29] reported that $\sum_{j=1}^{n} w_j = 1$.

Table 4 show the values of the calculated GRG, GRC and grey relational grade while Table 5 shows the resulting factor effects of the process factors with the values in bold representing the optimal level of process factor. Figure 5 shows the main effect plots obtained using the values presented in Table 5.

From Fig. 5, it can be observed that the optimum performing coconut shell-reinforced brake pad can be obtained using 14 MPa molding pressure (MP), 140 °C molding temperature (MT), 8 min curing time (CT) and 5 h heat treatment time (HTT) as optimal process parameters. This result is comparable with the earlier work of Abutu et al. [18] who reported an optimal process parameter of 14 MPa molding pressure, 160 °C molding temperature, 8 min curing time and 5 h heat treatment time using seashell as reinforcement material.

3.4 Characterization of commercial and optimized samples

Commercially available brake pad produced by Ibeto Group of Companies (control) and GRA-optimized samples were characterized to evaluate the performance of the samples in terms of mechanical and tribological properties. Experiments were conducted based on the optimized values obtained from GRA to validate the empirical regression models of the developed brake pad samples. The results compared with the control are summarized in Table 6.

As shown in Table 6, it can be seen that the performance of the optimized coconut shell-reinforced samples compared favorably with commercially available brake pad used as control. In addition, the experimental findings also indicate that the coefficient of friction of both brake pad samples fall within the category of class H ($\mu > 0.55$) type of brake pads [31], while the optimized samples showed better wear resistance compared to the control. The differences in the performance of the brake pad samples may be due to the variation in process parameters (production method) and constituent materials. Salmah et al. [32], reported that compared to mineral fillers, the inclusion of the lignocellulosic filler such as coconut shell powder in composite improves its wear resistance. Therefore, based on the tribology test results (wear rate and friction coefficient) presented in Table 6, it can be concluded that the optimized coconut shell-reinforced pad is capable of producing less noise and vibration during application. This is in line with earlier work of Rabia et al. [4], who found out that lower wear rate and stable coefficient of friction lead to reduced brake noise and vibration during braking. As a result, coconut shells are suitable eco-friendly replacement for asbestos in automotive brake pads.

3.5 Empirical regression models

The model equations of responses shown in Eqs. 22–28 were obtained with the aid of MINITAB 17 statistical software using the empirical data obtained from samples characterization. These models can be used to predict the properties of the friction materials. The optimal values of MP, MT, CT and HTT at 14 MPa, 140 °C, 8 min and 5 h, respectively, obtained from GRA as shown in Fig. 5 was used to determine the optimal response values of the coconut shell-reinforced brake pad. The notation w, x, y and z indicated in the equations represent the optimal values of MP, MT, CT and HTT, respectively. The percentage errors obtained during validation are shown in Table 7.

(1) Coefficient of friction

$$\begin{aligned} &\mu = 1.128 - 0.01223w - 0.000240x - 0.01056y - 0.0429z \\ &R\text{-sq} = 85.52\% \text{ and } R\text{-sq (adj)} = 75.62\% \\ &\mu = 0.624 \end{aligned} \tag{22}$$

(2) Wear rate

$$\begin{aligned} &\text{Wear rate (mg/m)} = 0.445 - 0.0011w \\ &\quad - 0.00592x + 0.0202y + 0.0607z \\ &R\text{-sq} = 66.77\% \text{ and } R\text{-sq (adj)} = 51.63\% \\ &\text{Wear rate} = 0.0659 \text{ mg/m}. \end{aligned} \tag{23}$$

(3) Ultimate tensile strength

$$\begin{aligned} &\text{UTS (MPa)} = 10.09 - 0.202w - 0.0043x + 0.221y - 0.251z \\ &R\text{-sq} = 79.61\% \text{ and } R\text{-sq (adj)} = 70.01\% \\ &\text{UTS} = 7.083 \text{ MPa} \end{aligned} \tag{24}$$

(4) Compressive strength

$$\begin{aligned} &\text{CS (MPa)} = 5.23 - 0.014w - 0.0147x + 0.099y - 0.020z \\ &R\text{-sq} = 60.56\% \text{ and } R\text{-sq (adj)} = 50.00\% \\ &\text{CS} = 3.668 \text{ MPa} \end{aligned} \tag{25}$$

(5) Hardness

$$\begin{aligned} &\text{Hardness} = 64.8 - 0.223w + 0.0361x + 1.055y - 0.39z \\ &R\text{-sq} = 75.14\% \text{ and } R\text{-sq (adj)} = 60.00\% \\ &\text{Hardness} = 61.96 \text{ Shore D scale} \end{aligned} \tag{26}$$

(6) Flexural strength

$$\begin{aligned} &F_S\text{(MPa)} = 11.8 + 0.001w - 0.0392x + 0.608y - 0.462z \\ &R\text{-sq} = 65.09\% \text{ and } R\text{-sq (adj)} = 56.93\% \\ &F_S = 8.880 \text{ MPa} \end{aligned} \tag{27}$$

Table 4 Results of GRG, GRC and grades

Scenario	GRG							GRC							Grade
	UTS	Compressive strength	Hardness	Flexural strength	Impact strength	Coefficient of friction	Wear rate	UTS	Compressive strength	Hardness	Flexural strength	Impact strength	Coefficient of friction	Wear rate	
X_o	1.00	1.00	1.00	1.00	1.00	1.00	1.00	–	–	–	–	–	–	–	–
1	0.70	0.57	0.57	0.65	0.52	1.00	0.72	0.62	0.54	0.54	0.59	0.51	1.00	0.64	0.6346
2	0.58	0.66	0.56	0.63	0.27	0.62	1.00	0.54	0.59	0.53	0.58	0.41	0.57	1.00	0.6031
3	0.86	0.73	0.54	1.00	0.63	0.72	0.59	0.78	0.65	0.52	1.00	0.57	0.64	0.55	0.6731
4	0.54	0.65	0.33	0.59	0.24	0.73	0.64	0.52	0.59	0.43	0.55	0.40	0.65	0.58	0.5305
5	1.00	1.00	1.00	0.94	0.58	0.72	0.67	1.00	1.00	1.00	0.90	0.54	0.64	0.60	0.8122
6	0.53	0.60	0.37	0.68	0.48	0.46	0.58	0.51	0.56	0.44	0.61	0.49	0.48	0.54	0.5197
7	0.76	0.67	0.57	0.44	0.33	0.46	0.80	0.67	0.60	0.54	0.47	0.43	0.48	0.72	0.5588
8	0.65	0.76	0.74	0.65	0.51	0.62	0.35	0.59	0.68	0.65	0.59	0.50	0.57	0.43	0.5739
9	0.00	0.31	0.00	0.22	0.07	0.34	0.90	0.33	0.42	0.33	0.39	0.35	0.43	0.84	0.4421
10	0.82	0.92	0.18	0.93	0.70	0.22	0.68	0.73	0.87	0.38	0.87	0.62	0.39	0.61	0.6392
11	0.87	0.70	0.42	0.24	0.53	0.73	0.47	0.79	0.62	0.46	0.40	0.51	0.65	0.48	0.5592
12	0.35	0.61	0.35	0.00	0.10	0.08	0.45	0.43	0.56	0.43	0.33	0.36	0.35	0.48	0.4211
13	0.85	0.86	0.69	0.82	0.91	0.31	0.90	0.77	0.79	0.62	0.73	0.84	0.42	0.83	0.7152
14	0.80	0.91	0.27	0.24	0.46	0.61	0.92	0.71	0.84	0.41	0.40	0.48	0.56	0.86	0.6085
15	0.19	0.94	0.38	0.70	0.61	0.35	0.90	0.38	0.89	0.45	0.63	0.56	0.43	0.84	0.5979
16	0.28	0.00	0.99	0.88	0.96	0.00	0.92	0.41	0.33	0.97	0.81	0.93	0.33	0.86	0.6630
17	0.86	0.70	0.32	0.22	0.39	0.67	0.60	0.79	0.63	0.42	0.39	0.45	0.60	0.56	0.5481
18	0.86	0.89	0.27	0.53	0.57	0.36	0.47	0.78	0.82	0.41	0.52	0.54	0.44	0.48	0.5689
19	0.72	0.88	0.37	0.66	0.55	0.51	0.90	0.64	0.81	0.44	0.59	0.53	0.51	0.83	0.6209
20	0.93	0.59	0.46	0.35	0.60	0.61	0.43	0.88	0.55	0.48	0.43	0.56	0.56	0.47	0.5622
21	0.36	0.68	0.38	0.08	0.00	0.62	0.21	0.44	0.61	0.45	0.35	0.33	0.57	0.39	0.4482
22	0.87	0.68	0.53	0.64	0.52	0.28	0.49	0.79	0.61	0.51	0.58	0.51	0.41	0.49	0.5577
23	0.94	0.89	0.57	0.66	0.56	0.82	0.00	0.90	0.82	0.54	0.60	0.53	0.74	0.33	0.6360
24	0.98	0.84	0.99	0.88	0.79	0.50	0.47	0.95	0.76	0.97	0.81	0.70	0.50	0.48	0.7403
25	0.90	0.95	0.86	0.76	0.69	0.11	0.92	0.83	0.91	0.79	0.68	0.62	0.36	0.86	0.7193
26	0.96	1.00	0.82	0.71	0.65	0.20	0.95	0.92	1.00	0.74	0.63	0.59	0.39	0.91	0.7375
27	0.93	0.96	0.84	0.73	0.77	0.18	0.94	0.87	0.92	0.75	0.65	0.69	0.38	0.89	0.7355

Table 5 Resulting factor effects of process factors (average GRG)

Factor	Axial points		Cubic points		Center point
	Level 1	Level 5	Level 2	Level 4	Level 3
MP	0.5481	0.5689	0.6241	0.569875	**0.6397**
MT	0.6209	0.5622	0.6218	0.572188	**0.6324**
CT	0.4482	0.5577	0.5629	0.63115	**0.6521**
HTT	0.636	**0.7403**	0.6132	0.580775	0.6109

(7) Impact strength

$$I_S(\text{J/mm}) = 0.01635 - 0.000017w + 0.000002x + 0.001075y + 0.001217z$$

$$R\text{-sq} = 77.44\% \text{ and } R\text{-sq (adj)} = 64.24\%$$

$$I_S = 0.029\,\text{J/mm} \quad (28)$$

As shown in Eqs. 22–28, it can be observed that the value of the correlation coefficient (R-sq_{adj}) falls below 80%. This may be due to noise which may result from experimental uncertainty.

3.6 Analysis of variance (ANOVA)

In order to identify the significant effects of process parameters, ANOVA was conducted. This analysis was carried out at 99% confidence level using 0.01 significance level (α). Equation 29 was used to calculate the sum of square (SS_{Total}) of individual responses. Tables 8, 9, 10, 11, 12, 13 and 14 shows the values of the calculated SS_{Total}, mean square (MS), f values, degree of freedom (DOF) and percentage contribution.

$$SS_{Total} = \sum_{i=1}^{N} k_i^2 - \frac{1}{N}(k_i)^2 \quad (i = 1, 2, 3 \ldots, 27) \quad (29)$$

Table 6 Experimental results compared with commercial product (control)

S/N	Properties	Commercial product (X)	Coconut shell-reinforced brake pad (C)
1.	Ultimate tensile strength (MPa)	5.071	7.38
2.	Bending strength (MPa)	8.41	8.34
3.	Hardness (shore D scale)	62.14	63.31
4.	Compressive strength (MPa)	5.451	3.817
5.	Impact strength (J/mm)	0.082	0.032
6.	Coefficient of friction	0.634	0.614
7.	Wear rate (mg/m)	0.04184	0.03156

where k = observations in ith sample and N = number of observation (N = 27).

The ANOVA for coefficient of friction and flexural strength shown in Tables 8 and 13 indicates that heat treatment time (HTT) with percentage contribution of 46.3 and 24.23%, respectively, has the highest significant effects on the performance of the brake pads. This result is contrary to the earlier work of Abutu et al. [18], who reported that the tribological properties of seashell-reinforced brake pads are mostly affected by the curing time (CT). Also, the ANOVA for ultimate tensile strength, compressive strength, hardness and impact strength shown in Tables 10, 11, 12 and 14 indicates that the mechanical properties of the developed brake pads are mostly influenced by curing time (CT), with percentage contribution of 30.38, 31.40, 29.13 and 47.75%, respectively. In addition, the effects of all the process factors on the performance of the developed brake pad are significant since their p values are greater than 0.010 (1%).

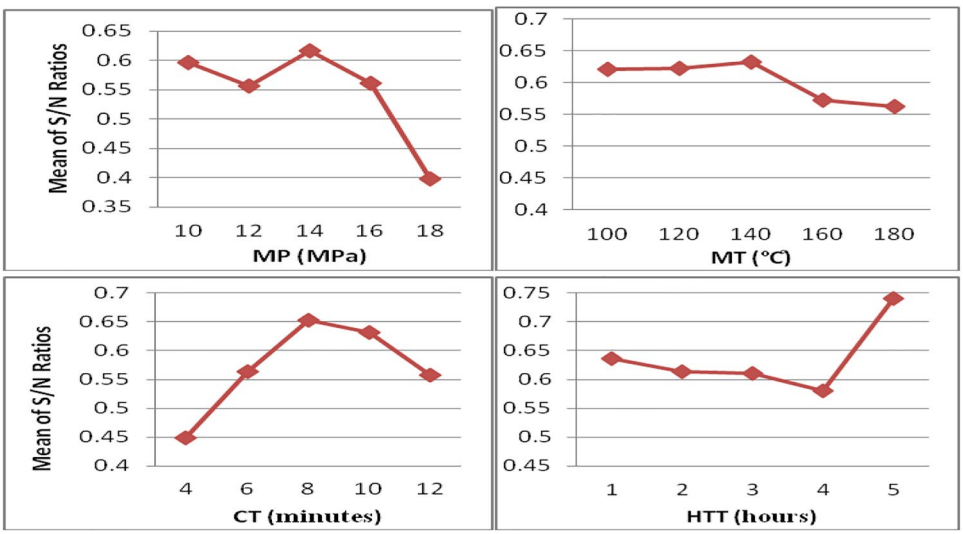

Fig. 5 Plots of factor effects

Table 7 Confirmation test percentage error

	Experimental value	Calculated value	Percentage error (*E*) %
Ultimate tensile strength (MPa)	7.38	7.083	4.02
Bending strength (MPa)	8.54	8.880	3.98
Hardness (shore D scale)	63.31	61.96	2.13
Compressive strength (MPa)	3.717	3.668	4.90
Impact strength (J/mm)	0.0302	0.029	3.97
Coefficient of friction	0.614	0.624	1.63
Wear rate (mg/m)	0.0315	0.0304	0.79

Table 8 ANOVA for coefficient of friction

Process factor	Degree of freedom	Sum of square	Mean square	*f* value	Contribution (%)
MP (MPa)	4	0.028	0.0069	4.986	18.08
MT (°C)	4	0.017	0.0044	3.148	11.41
CT (min)	4	0.023	0.0058	4.18	15.15
HTT (h)	4	0.071	0.0177	12.77	46.3
Error	10	0.014	0.0014		9.063
Total	26	0.153	0.0059		100

Table 9 ANOVA for wear rate

Process factor	Degree of freedom	Sum of square	Mean square	*f* value	Contribution (%)
MP (MPa)	4	0.492	0.123	12.365	17.65
MT (°C)	4	0.916	0.229	23.046	32.9
CT (min)	4	0.603	0.151	15.169	21.65
HTT (h)	4	0.675	0.169	16.975	24.23
Error	10	0.099	0.01		3.569
Total	26	2.786	0.107		100

Table 10 ANOVA for UTS

Process factor	Degree of freedom	Sum of square	Mean square	*f* value	Contribution (%)
MP (MPa)	4	21.77	5.4425	8.900	20.34
MT (°C)	4	22.46	5.615	9.181	20.99
CT (min)	4	33.61	8.4025	13.74	31.40
HTT (h)	4	23.07	5.7675	9.431	21.56
Error	10	6.116	0.6116		5.714
Total	26	107.0	4.1164		100

3.7 Contour and 3D surface plots

The contour and 3D surface plots for the properties of the coconut shell-reinforced brake pads are shown in Figs. 6a–g and 7a–g, respectively.

The contour plots shown in Fig. 6a–g indicate how change in two influential factors (most significant factors) affect the properties of the coconut shell-reinforced brake pad samples, while keeping other two factors constant. The contour levels shown in Fig. 6e–g revealed that hardness of > 70 Shore D, flexural strength > 17.5 MPa and impact strength > 0.035 J/mm can be achieved using CT of 10 min and HTT of 4.5 h. Also, the contour levels shown in Fig. 6c revealed that UTS > 6 MPa can be achieved using CT of 9 min and HTT of 2 h while Fig. 6d shows that compressive strength of > 5 MPa can be achieved using MT of 150

Table 11 ANOVA for compressive strength

Process factor	Degree of freedom	Sum of square	Mean square	*f* value	Contribution (%)
MP (MPa)	4	6.286	1.57	13.102	21.72
MT (°C)	4	7.866	1.97	16.395	27.17
CT (min)	4	8.433	2.11	17.577	29.13
HTT (h)	4	5.162	1.29	10.759	17.83
Error	10	1.199	0.12		4.144
Total	26	28.95	1.11		100

Table 12 ANOVA for hardness

Process factor	Degree of freedom	Sum of square	Mean square	*f* value	Contribution (%)
MP (MPa)	4	183.15	45.79	8.881	21.69
MT (°C)	4	103.16	25.79	5.003	12.22
CT (min)	4	256.50	64.13	12.44	30.38
HTT (h)	4	250.05	62.51	12.13	29.61
Error	10	51.552	5.155		6.105
Total	26	844.41	32.48		100

Table 13 ANOVA for flexural strength

Process factor	Degree of freedom	Sum of square	Mean square	*f* value	Contribution (%)
MP (MPa)	4	112.45	28.1	47.34	19.99
MT (°C)	4	71.6	17.9	30.14	12.73
CT (min)	4	170.05	42.5	71.58	30.23
HTT (h)	4	202.5	50.6	85.24	36.00
Error	10	5.94	0.60		1.06
Total	26	562.54	21.6		100

Table 14 ANOVA for impact strength

Process factor	Degree of freedom	Sum of square	Mean square	*f* value	Contribution (%)
MP (MPa)	4	0.940	0.235	4.68	17.60
MT (°C)	4	0.078	1.950	0.39	1.463
CT (min)	4	2.550	0.638	12.7	47.75
HTT (h)	4	1.270	0.318	6.33	23.78
Error	10	0.502	5.020		9.401
Total	26	5.340	0.205		100

°C and CT of 9 min. Finally, from Fig. 5b, it can be observed that a wear rate of 0–0.2 mg/m can be obtained using MP of 140 °C and HTT of 1.1 h while Fig. 6a shows that coefficient of friction > 0.8 can be achieved using MP of 10.5 MPa and HTT of 1.1 h. The 3D surface plots shown in Fig. 7a–g indicate how change in two influential factors (most significant factors) affects the properties of the coconut shell-reinforced brake pad samples.

4 Conclusion

This study presents the use of coconut shell as reinforcement material for the production of asbestos-free brake pad. The newly formulated brake pad was studied by investigating its performance (tribological and mechanical properties). Based on the results obtained, the following conclusions can be drawn:

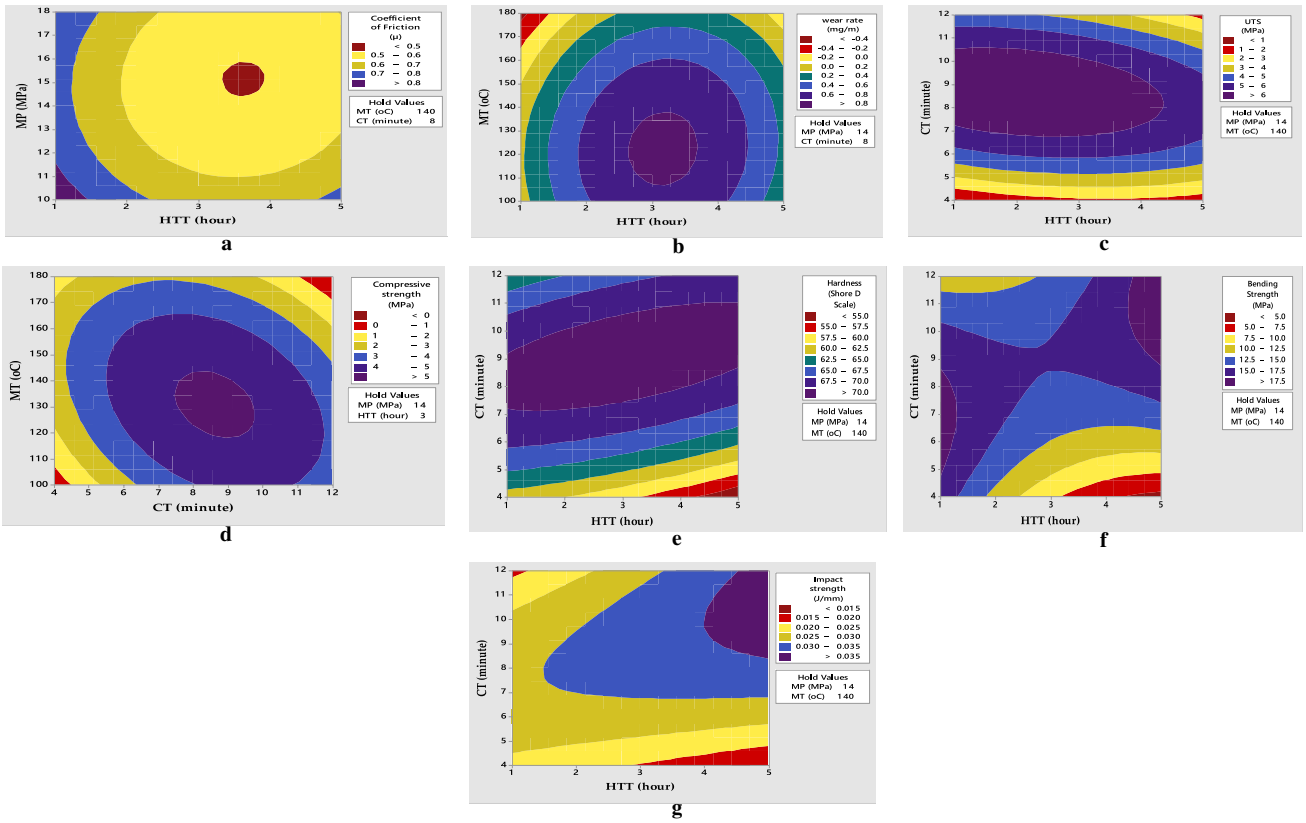

Fig. 6 Contour plots for **a** coefficient of friction, **b** wear rate, **c** ultimate tensile strength, **d** compressive strength, **e** hardness, **f** flexural strength, **g** impact strength

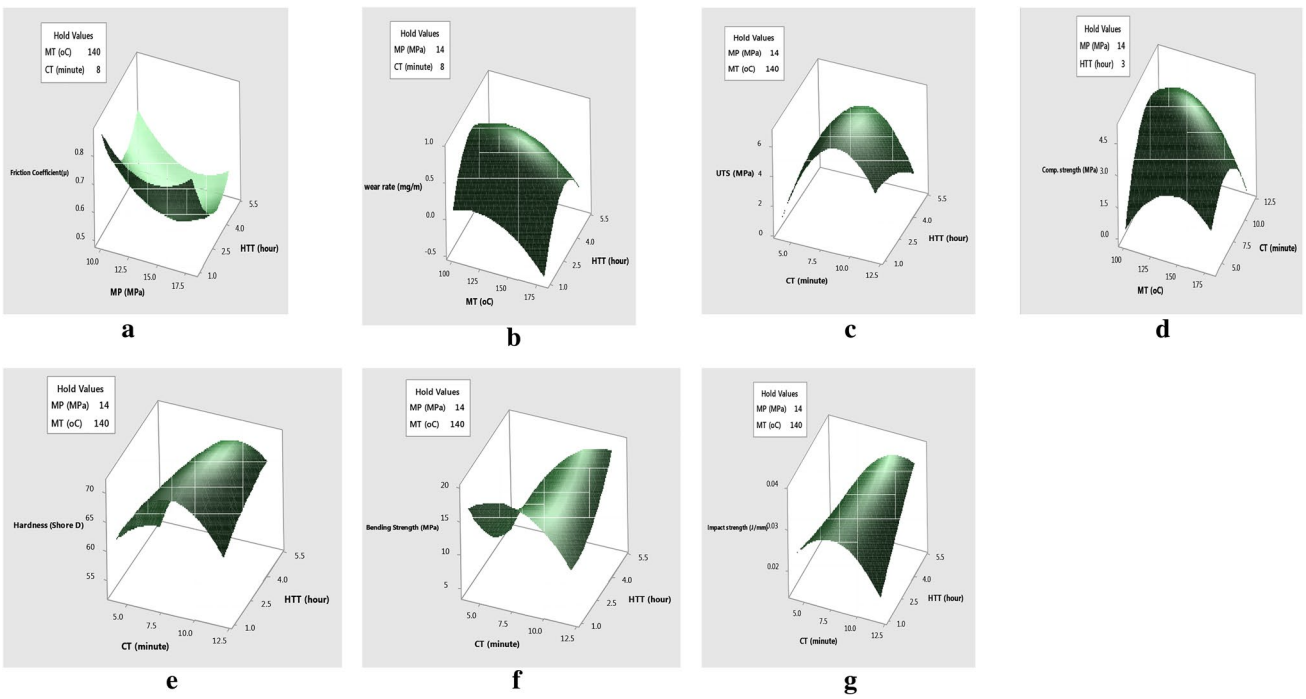

Fig. 7 3D surface plots for **a** coefficient of friction, **b** wear rate, **c** ultimate tensile strength, **d** compressive strength, **e** hardness, **f** flexural strength, **g** impact strength

(1) The performance of the developed brake pad changes as the process factor combination (MP, MT, CT and HTT) varies. As a result, the samples produced with different process factors gave varying performance values.
(2) Also, the optimal multi-response coconut shell-reinforced brake pad composite can be produced using molding pressure, molding temperature, curing time and heat treatment time of 14 MPa, 140 °C, 8 min and 5 h, respectively.
(3) Similarly, the multi-response optimization results revealed that the optimized and commercial brake pads fall within the class H (> 0.55) type of brake pads. As a result, can be recommended by SAE (Society of Automobile Engineers) for use in heavy duty automobile.
(4) The ANOVA results indicate that the mechanical and tribological properties of the developed material are mostly influenced by curing time and heat treatment time, respectively, while the confirmation test results obtained using the empirical models indicate that the percentage error of all responses falls below 5% indicating that the experimental processes possess a good accuracy.
(5) Finally, the optimal values of all responses fall within standard requirements of brake pads as it compared favorably with commercially available brake pads. Therefore, it can be concluded that the performance of the developed brake pad compares satisfactorily and is capable of producing less brake noise and vibration during braking due to its low wear rate and stable friction coefficient. Consequently, coconut shells can serve as a possible substitute for asbestos in brake pad production.

Acknowledgements The authors are grateful to the management of Federal University of Technology Minna—Nigeria for the Grant (Senate/FUTMINNA/2015/03) allocated to this research.

Funding This study was funded by Federal University of Technology, Minna—Nigeria (Senate/FUTMINNA/2015/03).

Compliance with ethical standards

Conflict of interest The authors declare that they have no conflict of interest.

References

1. Belhocine A, Wan ZWO (2018) Computational fluid dynamics modeling and computation of convective heat coefficient transfer for automotive disc brake rotors. Comput Therm Sci 10(1):1–21
2. Mohd RI, Rahim AAB, Belhocine A, Jamaludin MT, Wan ZWO (2016) Brake torque analysis of fully mechanical parking brake system: theoretical and experimental approach. Measurement 94:487–497
3. Belhocine A, Nouby MG (2015) Effects of material properties on generation of brake squeal noise using finite element method. Lat Am J Solids Struct 12:1432–1447
4. Rabia AM, Salem MM, Nouby MG, Ali MA (2013) Experimental study of automobile disc brake noise and vibration: a review. Int J Mod Eng Res (IJMER) 3(1):199–203. ISSN: 2249-6645
5. Singer I, Pollock H (1992) Fundamentals of friction. Kluwer Academic Publishers, Barunlage
6. Belhocine A (2017) FE prediction of thermal performance and stresses in an automotive disc brake system. Int J Adv Manuf Technol 89:3563–3578. https://doi.org/10.1007/s00170-016-9357-y
7. Belhocine A, Wan ZWO (2018) CFD analysis of the brake disc and the wheel house through air flow: predictions of Surface heat transfer coefficients (STHC) during braking operation. J Mech Sci Technol 32(1):481–490
8. Anon E (2004) Automotive brake repairs trends and safety issues. http://www.sirim.my/amtee/pm/brake.hltm. Accessed 10 Aug 2014
9. Norton RL (2001) Machine design: an integrated approach, 2nd edn. Addison Wesley Longman, Singapore
10. Ole-Von U, Staffan S, Reed D, Michael B (2005) Antimony in brake pads-a carcinogenic component? J Clean Prod 13:19–31
11. Lawal SA, Ugwuoke IC, Abutu J, Lafia-Araga RA, Dagwa IM, Kariim I (2016) Rubber scrap as reinforced material in the production of environmentally friendly brake pad. Ref Modul Mater Sci Mater Eng. https://doi.org/10.1016/B978-0-12-803581-8.04070-4
12. Ibhadode AOA, Dagwa IM (2008) Development of asbestos-free friction pad material from palm kernel shell. J Braz Soc Mech Sci Eng 30(2):166–173
13. Ikpambese KK, Gundu DT, Tuleu LT (2014) Evaluation of palm kernel fibers (PKFs) for production of asbestos-free automotive brake pads. J King Saud Univ Eng Sci 28(1):110–118
14. Aigbodion VS, Agunsoye JO, Hassan SB, Asuke F, Akadike U (2010) Development of Asbestos-free brake pad using bagasse. Tribol Ind 32(1):12–18
15. Idris UD, Abubakar IJ, Nwoye CI, Aigbodiun VS (2015) Eco-friendly asbestos free brake-pad: using banana peels. J Eng Sci 27:185–192
16. Ademoh AN, Adeyemi IO (2015) Development and evaluation of maize husks (asbestos-free) based brake pad. Ind Eng Lett IEL 5(2):67–80
17. Bala KC, Okoli M, Abolarin MS (2016) Development of automobile brake pad using pulverized cow hooves. Leonardo J Sci 15(28):95–108
18. Abutu J, Lawal SA, Ndaliman MB, Lafia-Araga RA, Adedipe O, Choudhury IA (2018) Effects of process parameters on the properties of brake pad developed from seashell as reinforcement material using grey relational analysis. Eng Sci Technol Int J. https://doi.org/10.1016/j.jestch.2018.05.014
19. Bashar D, Peter BM, Joseph M (2012) Effect of material selection and production of a cold-worked composite brake pad. J Eng Pure Appl Sci 2(3):23
20. Rowell RM (1998) The state of art and future development of bio-based composite science and technology towards the 21st century. In: Fourth Pacific Rim bio-based composites symposium, Indonesia, 2–5 November 1998, pp 1–18
21. Norazlina H, Fahmi ARM, Hafizuddin WM (2015) $CaCO_3$ from seashells as a reinforcing filler for natural rubber. J Mech Eng Sci 8:1481–1488

22. Askeland DR (1985) The science and engineering of materials. PWS Publishers, Boston
23. Chemiplastica (2010) Thermoset processing manual compression molding. http://www.chemiplastica.com/pdf/compression-molding-guidelines.pdf. Accessed 15 Mar 2015
24. Clara LN, Jane Maria FP, Mirabel CR (2005) Effect of the interfacial adhesion on the tensile and impact properties of carbon fiber reinforced polypropylene matrices. J Mater Res 8(1):1439–1516
25. Efendy H, Wan-Mochamad WM, Yusuf NBM (2010) Development of natural fiber in non-metallic brake friction material. In: Seminar Nasional Tahunan Teknik Mesin (SNTTM), 13–15, Ke-9 Palembang
26. Dagwa IM, Ibhadode AOA (2006) Some mechanical and physical properties of asbestos-free experimental brake pad. J Raw Mater Res (2). Available at http://www.scielo.br/scielo.php?script=sci_arttext&pid=S167858782008000200010&lng=en&nrm=iso&tlng=en. Accessed 12 Jan 2013
27. Belhocine A, Wan ZWO (2016) Three-dimensional finite element modeling and analysis of the mechanical behavior of dry contact slipping between the disc and the brake pads. Int J Adv Manuf Technol. https://doi.org/10.1007/s00170-016-8822-y
28. Belhocine A, Bakar ARA, Bouchetara M (2014) Structural and contact analysis of disc brake assembly during single stop braking event. Am J Mech Appl 2(3):21–28
29. Yiyo K, Taho Y, Guan WH (2008) The use of a grey-based Taguchi method for optimizing multi-response simulation problems. Eng Optim 40(6):517–552
30. Chin PF (2003) Manufacturing process optimization for wear property of fiber-reinforced polybutylene terephthalate composites with grey relational analysis. Wear 254:298–306
31. Blau PJ (2001) Compositions, testing and functions of friction brake materials and their additives. A report by Oak Ridge National Laboratory for U.S Dept. of Energy. Available at https://www.0rnl.gov/webworks/cppr/y2001/rpt/112956.pdf. Accessed 19 Jan 2013
32. Salmah H, Koay SC, Hakimah O (2013) Surface modification of coconut shell powder filled polylactic acid biocomposites. J Thermoplast Compos Mater 26(6):809–819